Remote Sens. **2015**, *7*, 14360-14385; doi:10.3390/rs71114360

OPEN ACCESS

remote sensing

ISSN 2072-4292

www.mdpi.com/journal/remotesensing

Article

Satellite Images for Monitoring Mangrove Cover Changes in a Fast Growing Economic Region in Southern Peninsular Malaysia

Kasturi Devi Kanniah [1,*], Afsaneh Sheikhi [1], Arthur P. Cracknell [2], Hong Ching Goh [3], Kian Pang Tan [1], Chin Siong Ho [4] and Fateen Nabilla Rasli [1]

[1] TropicalMap Research Group, Faculty of Geoinformation and Real Estate, UTM Palm Oil Research Centre, Universiti Teknologi Malaysia, Skudai, Johor 81310, Malaysia;
E-Mails: afsanehsheikhirs@gmail.com (A.S.); kptan2@live.utm.my (K.P.T.);
fanarapurply@gmail.com (F.N.R.)

[2] Division of Electronic Engineering and Physics, University of Dundee, Dundee DDI 4HN, UK;
E-Mail: apcracknell774787@yahoo.co.uk

[3] Department of Urban and Regional Planning, Faculty of Built Environment, Universiti Malaya, Kuala Lumpur 50603, Malaysia; E-Mail: gohhc@um.edu.my

[4] Department of Urban and Regional Planning, Faculty of Built Environment, Universiti Teknologi Malaysia, Skudai, Johor 81310, Malaysia; E-Mail: ho@utm.my

***** Author to whom correspondence should be addressed; E-Mail: kasturi@utm.my;
Tel.: +60-7553-0851 (ext. 30851).

Academic Editors: Chandra Giri, Ioannis Gitas and Prasad S. Thenkabail

Received: 6 August 2015 / Accepted: 13 October 2015 / Published: 29 October 2015

Abstract: Effective monitoring is necessary to conserve mangroves from further loss in Malaysia. In this context, remote sensing is capable of providing information on mangrove status and changes over a large spatial extent and in a continuous manner. In this study we used Landsat satellite images to analyze the changes over a period of 25 years of mangrove areas in Iskandar Malaysia (IM), the fastest growing national special economic region located in southern Johor, Malaysia. We tested the use of two widely used digital classification techniques to classify mangrove areas. The Maximum Likelihood Classification (MLC) technique provided significantly higher user, producer and overall accuracies and less "salt and pepper effects" compared to the Support Vector Machine (SVM) technique. The classified satellite images using the MLC technique showed that IM lost 6740 ha of mangrove areas from 1989 to 2014. Nevertheless, a gain of 710 ha of

mangroves was observed in this region, resulting in a net loss of 6030 ha or 33%. The loss of about 241 ha per year of mangroves was associated with a steady increase in urban land use (1225 ha per year) from 1989 until 2014. Action is necessary to protect the existing mangrove cover from further loss. Gazetting of the remaining mangrove sites as protected areas or forest reserves and introducing tourism activities in mangrove areas can ensure the continued survival of mangroves in IM.

Keywords: land cover change; mangroves; Iskandar Malaysia; remote sensing; maximum likelihood classifier; support vector machine

1. Introduction

Mangrove ecosystems are found in many sub-tropical and tropical areas of the world including Malaysia (Figure 1) and they are growing along sheltered coastlines such as river estuaries or tidal marshes [1]. The various goods and services provided by these forests make them one of the valuable ecosystems in the world. Although mangroves constitute less than 0.4% of the world's forests [2], they play an important role in providing habitats for thousands of marine and pelagic species, and serving the local communities with food, medicine, fuel and building materials. They also become important in mitigating the impact of climate change by sequestering CO_2 (the main greenhouse gas, apart from water vapor) from the atmosphere as they are one of the most carbon-rich forests in the tropics [3–5]. They also protect the coastal areas from tidal waves, tsunamis and cyclones [6].

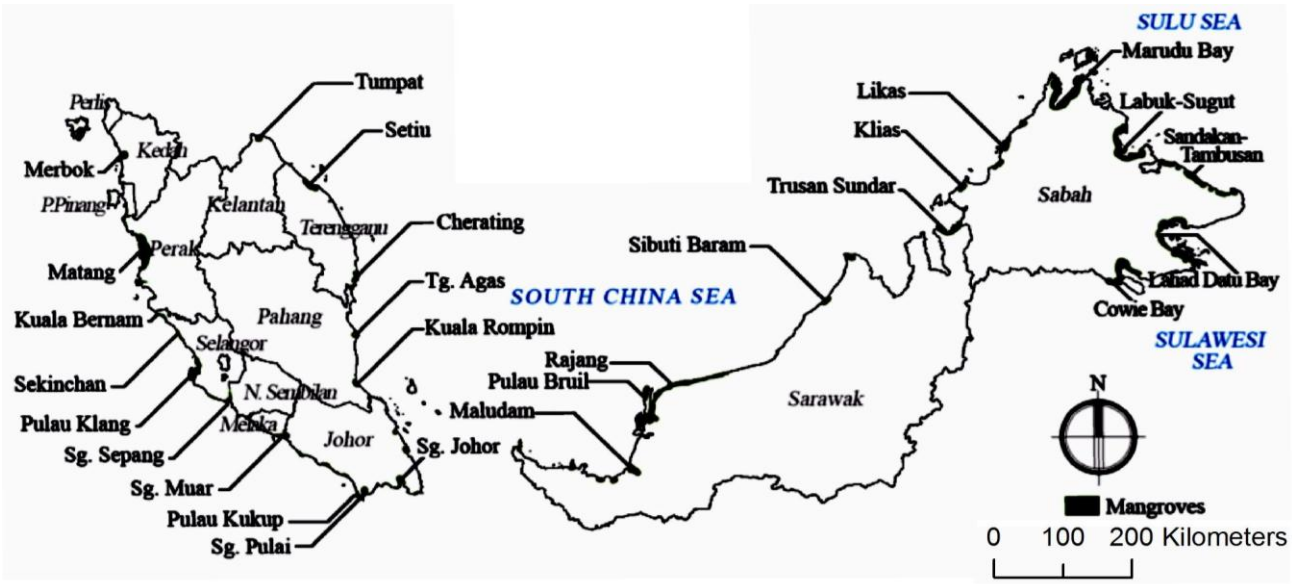

Figure 1. Mangrove forests distribution in Malaysia (Upper left: 7°22′46″N, 98°55′48″E and Lower right: 0°51′10″N, 119°16′00″E) [7].

Despite their significance in providing ecological and economic services, mangroves are being lost at the rate of about 1% per year globally [8]. The rate of loss is highest in developing countries and in Malaysia the rate is estimated to be about 1% or 1282 ha·year^{-1} since 1990 [9]. Mangroves are cleared

for coastal development, aquaculture, timber and fuel production [10]. Similar to the urbanization at global level, the southern coast of Johor-Iskandar Malaysia (IM) (Figure 2a) is undergoing the highest economic growth rate in the country. The fast pace urbanization threatens the survival of mangrove forests. In fact, Johor experienced the third largest mangrove loss after Selangor and Pahang states in Malaysia [11]. Mangrove forests in IM are continuously being cleared for constructing housing and industrial buildings, ports, power plants, oil storage, and a coastal way via massive reclamation works and also being transformed into urban water fronts.

Continuous loss of mangroves in this region will have a negative impact on environmental stability and on aquatic organisms and the biodiversity of the flora and fauna. Thus, an effective monitoring of mangrove forest is urgently required to prevent further loss of mangroves in Johor. Ground surveying methods and field observations are traditionally used for mapping mangrove areas. Although this can provide good mapping accuracy (cm to m), it is rather time consuming, laborious and costly; moreover, this method is not practical in a harsh mangrove environment that is temporarily inundated and hard to access [11,12]. Tidal change in mangrove areas makes the area change assessment more difficult by the inventory method. In past decades, multi temporal aerial photographs with high spatial resolution (<1 m) provided a local to sub-regional scale mapping and monitoring of mangrove ecosystems [13–15]. However, the potential for obtaining good images depends on flight and local weather conditions. Alternatively, remote sensing technology that delivers satellite images covering large-spatial scale, on a continuous basis (long-term) and at reduced cost can provide up to date information on mangrove forests, their spatio-temporal changes and the mangrove trees' health conditions. This information will provide economists, ecologists, and natural resources managers in Malaysia with valuable information to improve management strategies for mangrove ecosystems.

Remote sensing data and methods have been applied widely for mapping mangrove ecosystem distribution, species differentiation, health status, and changes of mangrove populations [1,11,16]. Satellite data with fine to medium spatial resolution such as Ikonos, Quickbird, and Landsat Thematic Mapper can provide adequate spatial details for mapping mangroves areas [16]. Meanwhile, hyperspectral images are useful in discriminating various mangrove species [17]. In Malaysia mangrove ecosystems have been studied using various remote sensing data for mangrove detection/areal delineation [18–21], mangrove change detection [22–29], mangrove species classification [21,30,31], and biomass of mangrove forest [5]. Change detection of mangrove areas using satellite data has been conducted in Malaysia at a local scale. However a detailed analysis of the Iskandar Malaysia region, using consistent data sources and methodology and suitable spatial and temporal scales, was not available. Thus, the overall goal of this study was to evaluate satellite imagery as a tool for monitoring changes in mangrove forests in Iskandar Malaysia and the secondary objective was to evaluate training sample size on classification accuracy. Both Maximum Likelihood Classifier (MLC) and Support Vector Machine (SVM) techniques were employed to classify mangrove and other land cover types in IM using time series Landsat Thematic Mapper (TM), Enhanced Thematic Mapper (ETM+) and Operational Land Imager (OLI) data. We then detected the changes in the land cover over a period of 25 years (1989–2014). Such studies are important for the development of a regional action plan in conserving mangrove resources in Malaysia.

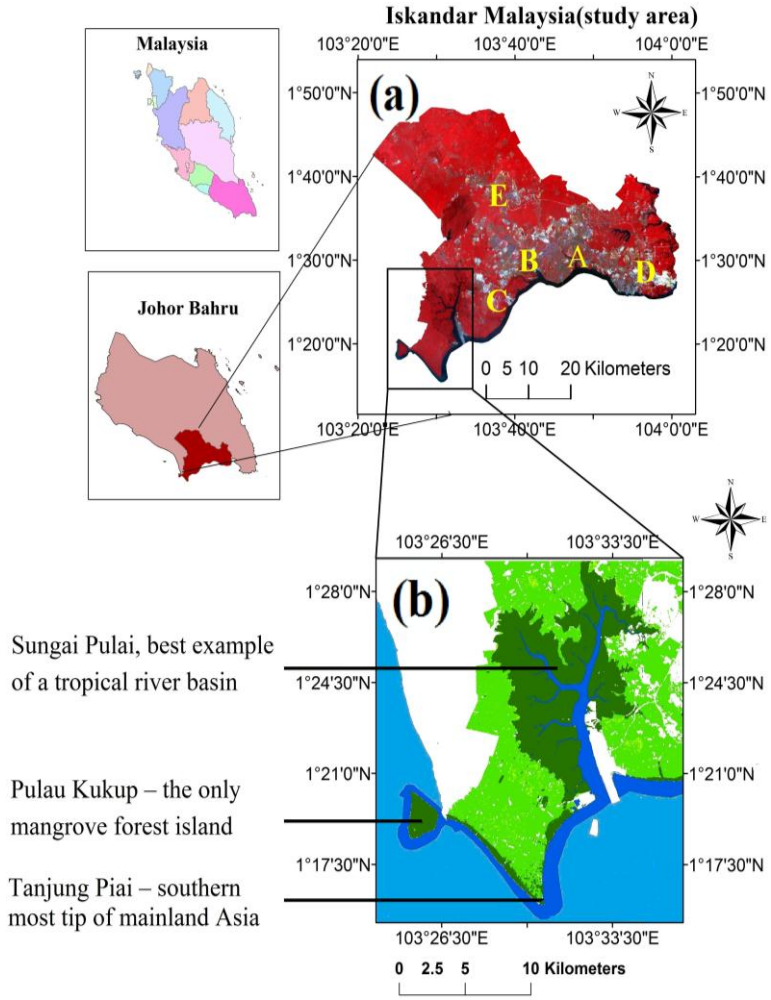

Figure 2. (**a**) The Iskandar Malaysia (IM) region in Johor State of Peninsular Malaysia shown by a Landsat image (the five flagship zones are marked as A–E); and (**b**) the three Ramsar sites in IM (source: Comprehensive Development Plan ii—unpublished).

2. Study Area

The total global coverage of mangrove forests is 15.62 Mha and of this 3.7% is found in Malaysia. Mangroves are established mostly along the west coast of Peninsular Malaysia and in the states of Sabah and Sarawak in Malaysian Borneo (Figure 1). Mangroves in Peninsular Malaysia constitute about 17% of the total mangroves of Malaysia (0.58 Mha) and the rest are found in Eastern Malaysia in Sabah (58.6%) and Sarawak (24.4%). The main mangrove tree species found in Malaysia are from the *Rhizophoraceae* family. However, there are at least a total of 70 mangroves species from 28 families that are found in this country [7]. Mangroves in Malaysia provide various ecological, economic and social benefits to the people and country [12].

This study focuses on Iskandar Malaysia (IM), the fastest growing national special economic region located in southern Johor, Malaysia (Figure 2a). It was established in 2006 to bring in more focused economic and infrastructure investments and the region is administered by the Iskandar Regional Development Authority (IRDA). The region encompasses an area of 2217 km^2; it involves five local

government authorities with five distinctive "Flagship Zones" or developmental focal points to guide its overall development (Figure 2a).

Currently the natural environment (forest, mangrove, rivers and water bodies) covers ~24% (56,719 ha) of the total IM (Comprehensive Development Plan ii—unpublished). The Ramsar Convention (formally the Convention on Wetlands of International Importance especially as Waterfowl Habitat) is an international treaty signed in 1971 for the conservation and sustainable utilization of wetlands; it came into force in 1975. There are over 2000 Ramsar sites worldwide of which 6 are in Malaysia, namely: Tasek Bera in Pahang, Kuching Wetlands National Park in Sarawak and Lower Kinabatangan-Segama Wetland in Sabah, while the other three are found in Johor in the IM region (see Figure 2b). Geographically, the mangrove forests in the region are distributed along the estuaries which can be broadly classified into three areas as shown in Figures 1 and 2b. Pulau Kukup, Sungai Pulai and Tanjung Piai (Tg Piai) mangrove areas (Figure 2b) found in IM were designated as Ramsar Sites in 2003. Mangrove forests are important in this region for shoreline protection, ecology, bio-diversity and as a source of income for local people.

3. Data and Methodology

We downloaded several scenes of Landsat Thematic Mapper (TM), Enhanced Thematic Mapper (ETM) and Operational Land Imager (OLI) images from the United States Geological Survey (USGS) website, available for free at [32]. The images covered 1989, 2000, 2005, 2007, 2009, 2013 and 2014 of Johor state in Peninsular Malaysia. These periods were chosen because during the 1980s a new economic policy was implemented in Malaysia where the government focused on urbanization and industrialization that caused major changes in land cover. Data from the 2000s were important, because the growth of the Iskandar Malaysia (IM) region started in 2006 and massive developments are still continuing now.

The total cloud cover of the study area in each scene was not more than 20% (Table 1). The images were subset to the IM region (Figure 2) and the digital numbers were converted to reflectance following the method provided in the NASA Landsat 7 Science Data Users Handbook, available at [33]. Clouds were masked out based on the brightness temperature information of the Landsat thermal band. We calculated and examined the brightness temperature [34] of clouds in each image and masked them out by using the thresholds as shown in Table 1. Clouds are assumed to be colder than these thresholds [35]. We did not perform atmospheric correction because the images were not too hazy and the training data is from the image to be classified [36]. We ran a co-occurrence matrix texture measurement mean filter 3×3 window by using ENVI software (Exelis Visual Information Solutions, Boulder, Colorado) to smooth the spatial variation in the study area and thus improve the classification results [37].

Table 1. Cloud coverage and brightness temperature threshold values used to mask out clouds in Landsat images.

Landsat Images	Cloud Coverage (%)	Brightness Temperature (℃)
13 September 1989	6	<16
28 April 2000	10	<17
4 May 2005	2	<16
10 May 2007	5	<17
8 February 2009	0	-
27 June 2013	10	<18
13 May 2014	20	<18

There are over a dozen image classification algorithms that have come into use in recent years. Li *et al.* [38] carried out extensive tests on the performance of 15 of these algorithms and concluded that "when sufficiently representative training samples were used most algorithms performed reasonably well." To classify the Landsat images in our data set we have chosen two of the most commonly used of these algorithms, namely the Maximum Likelihood Classification (MLC), because it is simple, and the Support Vector Machine (SVM), because it is widely held to be "better" than other algorithms [39]. MLC uses a parametric logic which assumes that the data is normally distributed and the classes are trained based on the probability density function [40]. The probability of each pixel belonging to any particular class is calculated, and then the pixel is assigned to the class with the highest probability. SVM uses a non-parametric machine learning logic where no assumption is made on the data distribution [39]. SVM discriminates the data into a discrete number of classes by projecting the data into a feature space with hyperplanes by using a kernel function. Machine learning involves iterations to find the finest border line to discriminate the data. It was reported that the result of SVM is promising even with limited training samples [39].

We selected training samples from the images (Figure 3) by carefully selecting homogeneous pixels so that every land use/land cover (LULC) class (forest, oil palm, rubber, mangrove, urban, and water bodies) has three sets of training samples (10, 20 and 30 polygons where each polygon contains about 40–60 pixels). The number of pixels (40 or 60) selected for each polygon is dependent on the size of the land use. For example larger number of pixels was selected for oil palm and fewer pixels were used for rubber. Different training samples (10, 20 and 30 polygons) were used to test if MLC and SVM can produce higher accuracy with increased number of training samples. This size of training samples follows the guide where training sample size for each class should be not fewer than 10–30 times the number of bands [40]. We used all the spectral bands of Landsat sensors except for the thermal band for the classification with both MLC and SVM. For SVM we tested all kernel types *i.e.*, radial, polynomial, linear, and sigmoid [41] and after several trials we chose values of the following parameters that produced the highest accuracies (Bias in Kernel function = 1, Gamma in Kernel function = 0.167, penalty parameter = 100, pyramid level = 0 and class probability threshold = 0). The overall classification accuracies produced by MLC and SVM using 10, 20 and 30 samples were compared using Analysis of Variance (ANOVA).

The classification results were validated using another independent set of polygons (10 polygons with 40 to 60 pixels—Figure 3) distributed across the study region which we referred to the Johor land

use maps produced by the Department of Agriculture, Peninsular Malaysia (scale 1: 250,000) of 1990, 2000, 2006, 2008 and 2010. Similar to the training dataset we selected more validation pixels for oil palm and fewer pixels for rubber. The Johor land use maps were considered as ground-truth because these maps were produced from aerial photos and SPOT images, and verified by extensive field work. Our local knowledge of several locations also helped us to verify the results. We also used land cover reports produced by the Comprehensive Development Plan ii (unpublished) report produced by the Iskandar Regional Development Authority (IRDA) for years 2013 to 2025. Relative Predictive Error (RPE) was used in this study to quantify the mean percentage difference between land cover classified by digital classification techniques and land cover data produced by the Department of Agriculture (DOA) and IRDA. RPE provides the direction of changes (underestimation or overestimation) in predicted values compared to measured values.

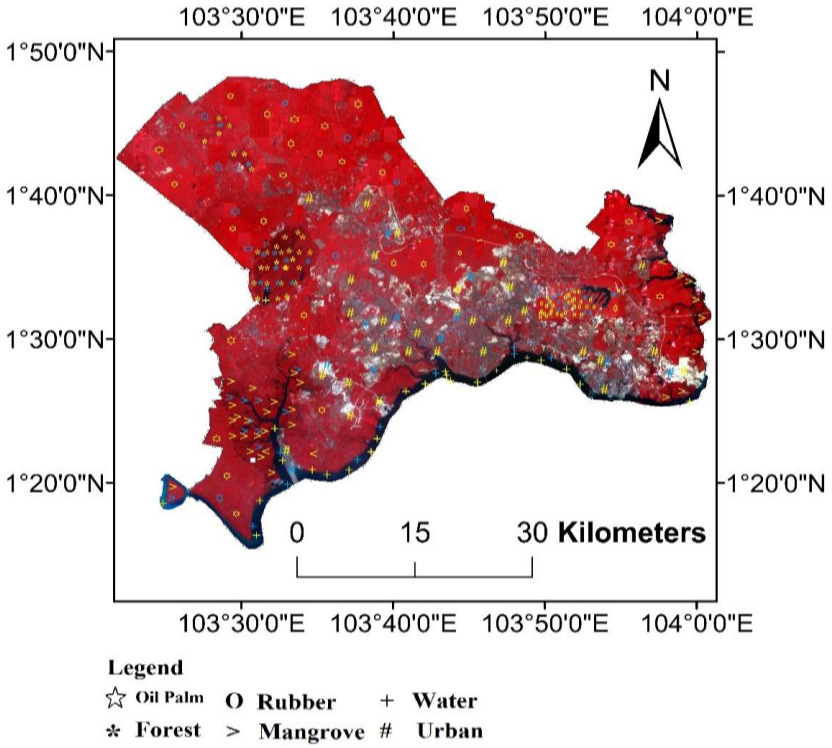

Figure 3. The distribution of test samples (30 polygons) and validation samples (10 polygons) for each land cover types in the study area. Yellow color symbols show the test samples and blue color represents the validation samples respectively.

The accuracy of the classified images was assessed using confusion matrices and kappa coefficients [42]. The overall accuracy in the confusion matrix is calculated by summing the number of pixels classified correctly and dividing by the total number of pixels. The kappa coefficient is calculated from [42] as follows:

$$\widehat{K} = \frac{N\sum_{i=1}^{r} x_{ii} - \sum_{i=1}^{r}(x_{i+} * x_{+i})}{N^2 - \sum_{i=1}^{r}(x_{i+} * x_{+i})} \quad (1)$$

where $\widehat{K}$ is the KHAT statistic (an estimate of KAPPA), r is the number of rows in the matrix, x_{ii} is the number of observations in row i and column i, x_{i+} and x_{+i} are the marginal totals of row i and column i,

respectively, and *N* is the total number of observations [42].Since the classified images suffered from the "salt and pepper" effect we ran post classification to remove these pixels. We used clump classes from the post-classification in the ENVI software (Exelis Visual Information Solutions, Boulder, Colorado) to clump closest and similarly classified areas. The pixels in 3×3 window size were clumped together by first carrying out a dilate operation then an erode operation on the classified image.

The classified images with highest overall accuracy and Kappa coefficient were selected to calculate the total area covered by each LULC types. We created shape files with a polygon feature for each LULC type using ArcCatalog software. All the LULC boundaries were delineated and their total areas were calculated.

4. Results

In this section we report the accuracy of each of the classification techniques used to classify various land use/land cover classes (LULC) in IM. This is followed by the change detection of the LULC between 1989 and 2014.

4.1. Classification Accuracy

A total of six LULC classes (forest, oil palm, rubber, mangrove, urban, and water bodies) were classified using the MLC and SVM classification techniques. The classification accuracy (Producer, User, Overall accuracies and the Kappa coefficient) is shown in Table 2 and for SVM the classification results with the highest accuracy obtained with radial functions are reported. Generally the classification run using 30 polygons yielded higher overall accuracy compared to 20 and 10 polygons. The overall accuracy of the images range between 62% (for SVM run on the image dated 2007 using 10 polygons) and 95% (for MLC run on the images dated 2000 and 2009 using 20 and 30 polygons respectively). The Kappa values for classifications using 30 samples range between 0.74 and 0.84 for SVM and from 0.85 to 0.93 for MLC. These values represent the general precision that can be expected in mapping land cover using the classification techniques.

Table 2. The user and producer accuracies of Landsat imageries using Maximum Likelihood (MLC) and Support Vector Machine (SVM) classification techniques. SVM R refers to the Radial function of SVM.

Year	Classification	Sample Size	Forest		Oil Palm		Rubber		Mangrove		Urban		Water Body		Overall Accuracies	
		(Polygons)	PA (%)	UA (%)	PA (%)	UA (%)	PA (%)	UA (%)	PA (%)	UA (%)	PA (%)	UA (%)	PA (%)	UA (%)	OA (%)	Kappa
1989	SVM R	10	68.71	90.10	47.49	43.18	76.03	85.96	90.76	96.13	53.94	40.54	98.25	86.36	71.51	0.65
1989	MLC	10	74.09	96.82	36.14	57.55	82.79	98.45	95.34	75.75	66.95	40.33	97.98	100.00	73.86	0.70
1989	SVM R	20	60.59	93.86	45.54	41.14	77.34	83.73	92.48	92.61	57.64	40.28	98.38	86.89	70.09	0.63
1989	MLC	20	77.67	96.96	44.89	42.23	75.82	8.86	82.31	99.05	67.18	39.43	98.11	100.00	73.10	0.67
1989	SVMR	30	53.54	97.50	83.69	54.97	79.31	71.32	98.32	99.25	96.20	99.56	100.00	97.22	81.53	0.77
1989	MLC	30	67.30	66.20	74.46	90.03	99.43	85.86	100.00	94.88	100.00	92.76	100.00	100.00	89.22	0.85
2000	SVM R	10	84.01	96.71	99.76	62.83	1.53	10.29	99.07	99.78	85.38	100.00	100.00	100.00	86.54	0.83
2000	MLC	10	90.74	98.96	99.20	78.54	58.82	97.83	99.86	99.08	97.08	100.00	100.00	100.00	94.07	0.93
2000	SVM R	20	84.45	96.80	99.28	72.06	54.68	49.70	99.57	99.29	62.46	100.00	100.00	99.87	87.43	0.84
2000	MLC	20	91.81	99.18	98.72	81.47	71.68	98.21	99.86	99.22	96.26	100.00	100.00	100.00	95.08	0.94
2000	SVMR	30	95.74	34.13	100.00	30.26	65.77	80.10	87.78	99.96	72.84	98.29	98.86	99.83	83.50	0.79
2000	MLC	30	89.85	84.84	93.22	87.21	83.94	92.42	87.85	87.60	75.51	95.84	98.15	99.00	89.83	0.86
2005	SVM R	10	83.95	96.36	98.24	59.96	0.00	0.00	99.64	93.42	72.73	100.00	99.73	100.00	85.11	0.82
2005	MLC	10	78.51	93.28	91.98	71.15	55.77	89.51	96.06	98.31	99.18	91.97	97.44	94.64	88.49	0.86
2005	SVM R	20	70.69	98.50	99.28	65.16	46.84	96.85	99.00	93.13	92.61	100.00	100.00	99.73	87.35	0.84
2005	MLC	20	65.80	95.22	98.56	68.51	78.00	97.81	99.57	97.89	99.76	98.44	99.73	100.00	89.31	0.87
2005	SVMR	30	83.32	57.58	79.65	83.30	84.64	80.49	73.89	100.00	100.00	99.84	100.00	97.72	85.88	0.82
2005	MLC	30	96.51	68.42	87.74	98.04	98.21	65.77	94.68	98.35	100.00	99.40	99.66	100.00	92.42	0.89
2007	SVM R	10	80.23	48.08	95.75	55.79	0.00	0.00	4.15	61.70	72.75	96.28	99.46	96.22	61.77	0.52
2007	MLC	10	77.62	94.36	94.39	71.33	57.52	91.03	95.85	98.24	99.06	92.37	97.44	95.26	88.81	0.86
2007	SVM R	20	64.69	96.86	97.91	56.95	0.00	0.00	96.92	92.10	78.83	97.54	99.73	92.28	79.82	0.75
2007	MLC	20	80.99	95.72	93.99	80.77	79.08	91.21	95.20	97.36	99.53	90.92	97.31	91.29	91.06	0.89
2007	SVMR	30	45.26	96.09	74.25	75.02	73.47	51.22	98.30	92.02	84.93	77.50	98.63	100.00	79.63	0.74
2007	MLC	30	67.20	90.07	89.20	87.82	88.63	88.37	94.18	93.13	87.16	70.70	98.54	100.00	89.26	0.86

Table 2. *Cont.*

Year	Classification	Sample Size (Polygons)	Forest		Oil Palm		Rubber		Mangrove		Urban		Water Body		Overall Accuracies	
			PA (%)	UA (%)	PA (%)	UA (%)	PA (%)	UA (%)	PA (%)	UA (%)	PA (%)	UA (%)	PA (%)	UA (%)	OA (%)	Kappa
2009	SVM R	10	71.76	94.57	86.37	63.32	54.25	60.73	95.70	100.00	90.29	93.01	100.00	92.53	84.58	0.81
2009	MLC	10	85.47	96.98	91.82	72.15	48.15	97.79	96.28	100.00	100.00	90.76	99.46	93.78	90.04	0.88
2009	SVM R	20	63.58	96.72	90.14	58.33	53.16	61.31	95.70	98.60	82.46	93.25	100.00	92.41	82.12	0.78
2009	MLC	20	94.54	92.37	83.96	88.43	88.02	98.54	95.56	99.85	100.00	87.60	99.60	97.75	93.53	0.92
2009	SVMR	30	81.51	96.89	98.77	74.86	47.79	85.81	93.81	99.45	99.82	99.72	99.96	100.00	88.62	0.84
2009	MLC	30	88.95	94.43	94.31	92.34	97.61	100.00	98.24	94.62	85.22	86.61	99.84	99.84	94.61	0.93
2013	SVM R	10	31.81	87.42	87.95	56.81	9.80	90.00	98.42	67.06	90.88	94.07	97.01	99.20	73.14	0.67
2013	MLC	10	83.71	78.76	79.54	84.72	47.06	96.43	98.42	87.13	98.36	83.85	83.33	100.00	85.67	0.82
2013	SVM R	20	71.06	91.51	88.22	65.23	38.34	87.56	99.86	87.78	90.99	95.23	98.27	99.21	84.75	0.81
2013	MLC	20	95.66	87.88	85.30	89.58	68.85	99.68	100.00	98.59	99.30	89.37	94.65	99.83	92.97	0.91
2013	SVMR	30	81.51	96.89	98.77	74.86	47.79	85.81	93.81	99.45	99.82	99.72	99.96	100.00	80.98	0.75
2013	MLC	30	75.23	87.23	98.77	74.86	100.00	96.89	93.27	95.04	83.02	79.12	89.32	100.00	91.02	0.88
2014	SVM R	10	74.03	86.66	63.95	77.49	70.37	36.41	99.71	84.36	60.94	88.76	97.85	100.00	79.00	0.74
2014	MLC	10	78.54	97.64	80.60	91.77	93.46	96.40	99.71	86.46	98.71	68.51	77.66	100.00	87.80	0.85
2014	SVM R	20	72.91	85.20	85.73	64.05	26.36	99.18	99.93	83.23	79.06	87.91	97.04	100.00	81.88	0.78
2014	MLC	20	75.16	97.89	86.83	79.02	80.61	99.73	99.86	87.07	96.14	74.32	80.35	100.00	87.15	0.84
2014	SVMR	30	78.47	88.89	67.70	94.87	69.63	8.43	96.74	97.78	99.80	97.21	100.00	99.87	79.17	0.71
2014	MLC	30	85.88	100.00	86.70	87.17	92.31	81.08	86.15	96.55	94.64	77.37	85.42	100.00	88.37	0.85

PA = Producer's accuracy; UA = User's accuracy; OA = overall accuracy; MLC = Maximum Likelihood Classifier; SVM = Support Vector MachineOverall, MLC yielded the highest overall classification accuracy compared to SVM for all the seven years considered in this study and we found increasing the number of polygons increases the overall accuracy for both classifications methods (Figure 4). The results of analysis of variance (ANOVA or F test) showed that there is a significant difference between MLC and SVM for 10 (n = 7, p = 0.04, F value = 5.26), 20 (n = 7, p = 0.08, F value = 3.73) and 30 (n = 7, p = 0.0003, F value = 26.12) samples. The larger the sampling size especially from 10 samples to 30 samples the p value becomes smaller indicating the highly significant difference in the overall classification accuracy. A larger sample size with the same sample mean will result in a smaller p-value. However, the higher p value for 20 sample size compared to 10 sample size maybe due to the dissimilar sample mean between 10 and 20 sample sizes.

Water body and mangrove produced higher user and producer accuracies among the land cover classes where >76% of all pixels classified as water and mangrove are indeed water and mangrove on the ground (Table 2). An exception was found for mangrove classified by SVM images dated 2007 where the user and producer accuracies are 62% and 4% respectively. Forest class also produced higher user and producer accuracies (>65%) except for user accuracy for SVM year 2000, 2005, 2007 and producer accuracy of only 46% by SVM for year 2007. Meanwhile, rubber class produced very low (up to 0%) user and producer accuracies for some of the data (images dates 2000, 2005 and 2007) and interestingly this is only for the SVM technique. MLC however, produced higher user and producer accuracies compared to SVM technique (Table 2). The low accuracies for the rubber class may be attributed to the spectral similarity of rubber with forest with the 30 m resolution of Landsat which may have hindered the discrimination of rubber from forest class.

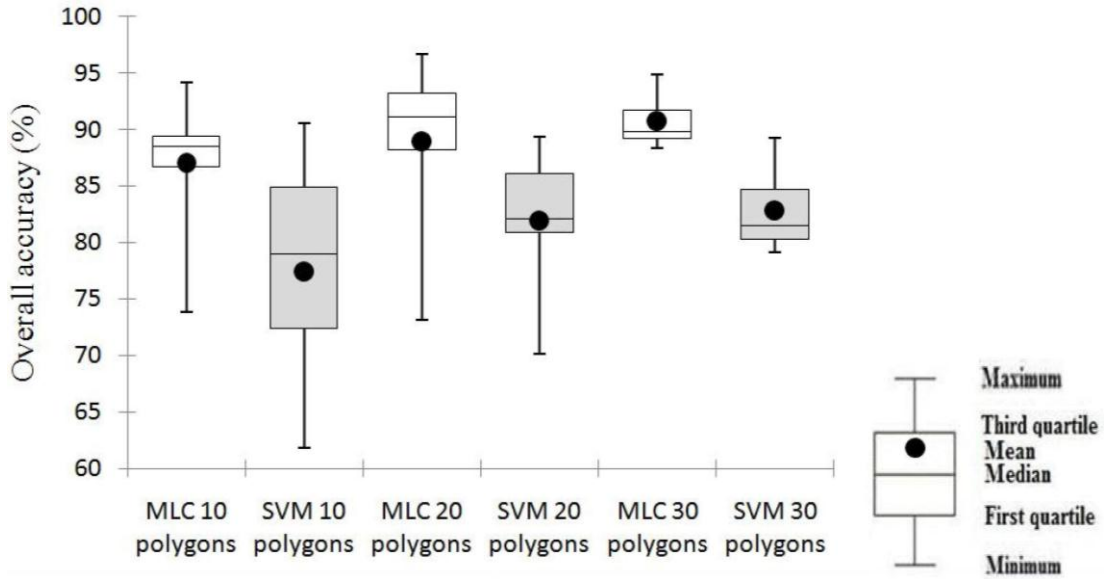

Figure 4. Boxplots showing the overall accuracy of Maximum Likelihood (MLC) and Support Vector Machine (SVM) classification techniques using 10, 20 and 30 polygons/sample sizes. The horizontal line in each of the boxes is the median, the black dot is the mean, the boxes are the first and third quartiles and the whiskers are the minimum and maximum values.

In order to assess the performance of each classifier to delineate the boundaries between the various land cover classes a few subsets of areas containing forest, mangrove, rubber and urban classes were zoomed (Figure 5) and it was found that the MLC technique run using 30 polygons produced fewer mixed pixels than SVM run using 30 polygons. For example Figure 5a shows more oil palm pixels within the forested area in the image classified by SVM compared to MLC. Similarly, in Figure 5b a large number of rubber pixels are found within the mangrove area in images classified by the SVM technique. In an area where there should be more rubber, like in Figure 5c, SVM produced about 1000 ha less rubber compared to the results of MLC. In Figure 5d with SVM we found some rubber pixels in the urban area (Johor Bahru) which is not true and MLC correctly captured this and shows no rubber within the urban area.

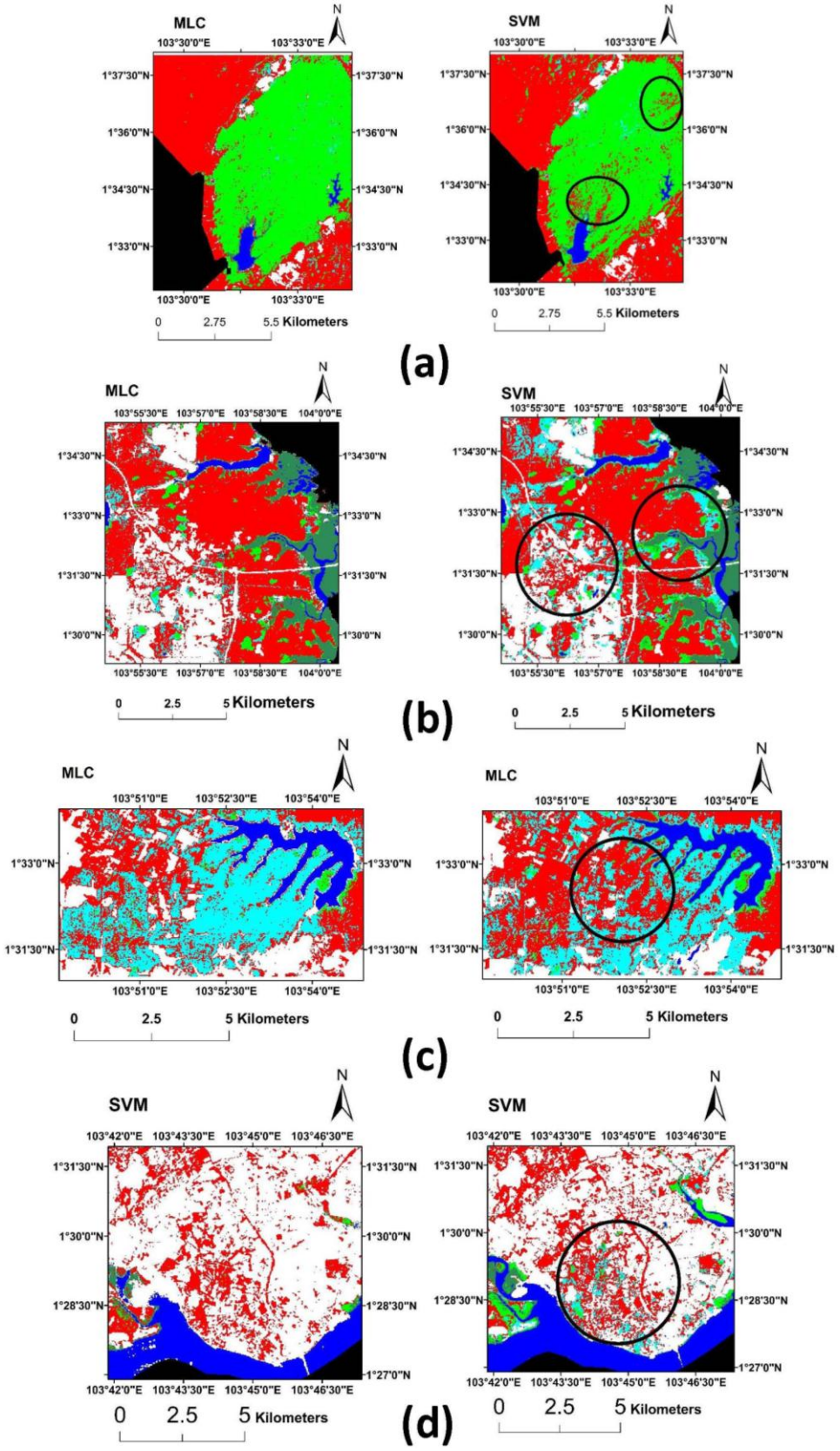

Figure 5. Subsets of images (2009) as classified by Maximum Likelihood Classification and Support Vector Machine techniques using 30 samples covering (**a**) Forest; (**b**) Mangrove; (**c**) Rubber; and (**d**) Urban areas in Iskandar Malaysia. The circles show "salt and pepper" effect on images classified by SVM compared to MLC techniques.

Table 3. Comparison between land use/land cover (LULC) produced by Maximum Likelihood Classification technique, land use map produced by the Department of Agriculture Malaysia (DOA) and the Comprehensive Development Plan (CDP) ii (unpublished). RPE (Relative Predictive Error) quantifies the mean percentage difference between land cover classified by MLC and land cover produced by DOA and IRDA. RPE provides the direction of changes (underestimation (negative sign) or overestimation (positive sign)) in predicted values compared to measured values.

Land Use Types	MLC 1989 (ha)	Land Use (DOA) 1990 (ha)	RPE (%)	MLC 2000 (ha)	Land Use (DOA) 2000 (ha)	RPE (%)	MLC 2005 (ha)	CDP 2005 (ha)	RPE (%)	MLC 2009 (ha)	Land Use (DOA) 2010 (ha)	RPE (%)
Forest	19,396	17,872	9	19,186	15,620	16	6720	6879	−1	6829	6612	3
Oil Palm	82,452	77,343	7	114,139	113,110	2	117,715	/	/	117,826	120,879	−3
Mangrove	18,403	17,046	8	15,066	17,460	−24	13,977	13,498	5	13,942	12,608	11
Urban	29,728	30,112	−2	37,201	36,360	3	51,294	/	/	53,306	52,998	1
Rubber	46,443	50,559	−9	9,272	12,450	−6	2768	/	/	4629	3291	41
Water	13,203	15,099	−13	13,099	13,000	1	12,571	12,401	1	11,471	11,046	4
Forest + Mangrove	37,799	34,918	1	34,252	33,091	3	20,697	20,377	1	20,753	19,220	8
Oil palm + Rubber	128,895	127,902	9	123,411	125,573	−2	120,483	119,302	1	122,455	124,170	−1

	MLC 2013 (ha)	CDP 2012 (ha)	RPE (%)	MLC 2014 (ha)	CDP 2012 (ha)	RPE (%)
Forest	6829	6879	−1	6828	6879	−1
Oil Palm	115,042	/	/	114,744	/	/
Mangrove	12,434	12,606	−1	12,733	12,606	−1
Urban	60,110	56,138	7	60,354	56,138	8
Rubber	1661	/	/	2043	/	/
Water	12,050	37,234	−68	11,467	37,234	−69
Forest + Mangrove	19,263	19,485	−1	19,132	19,485	−2
Oil palm + Rubber	116,703	95,508	22	116,787	95,508	22

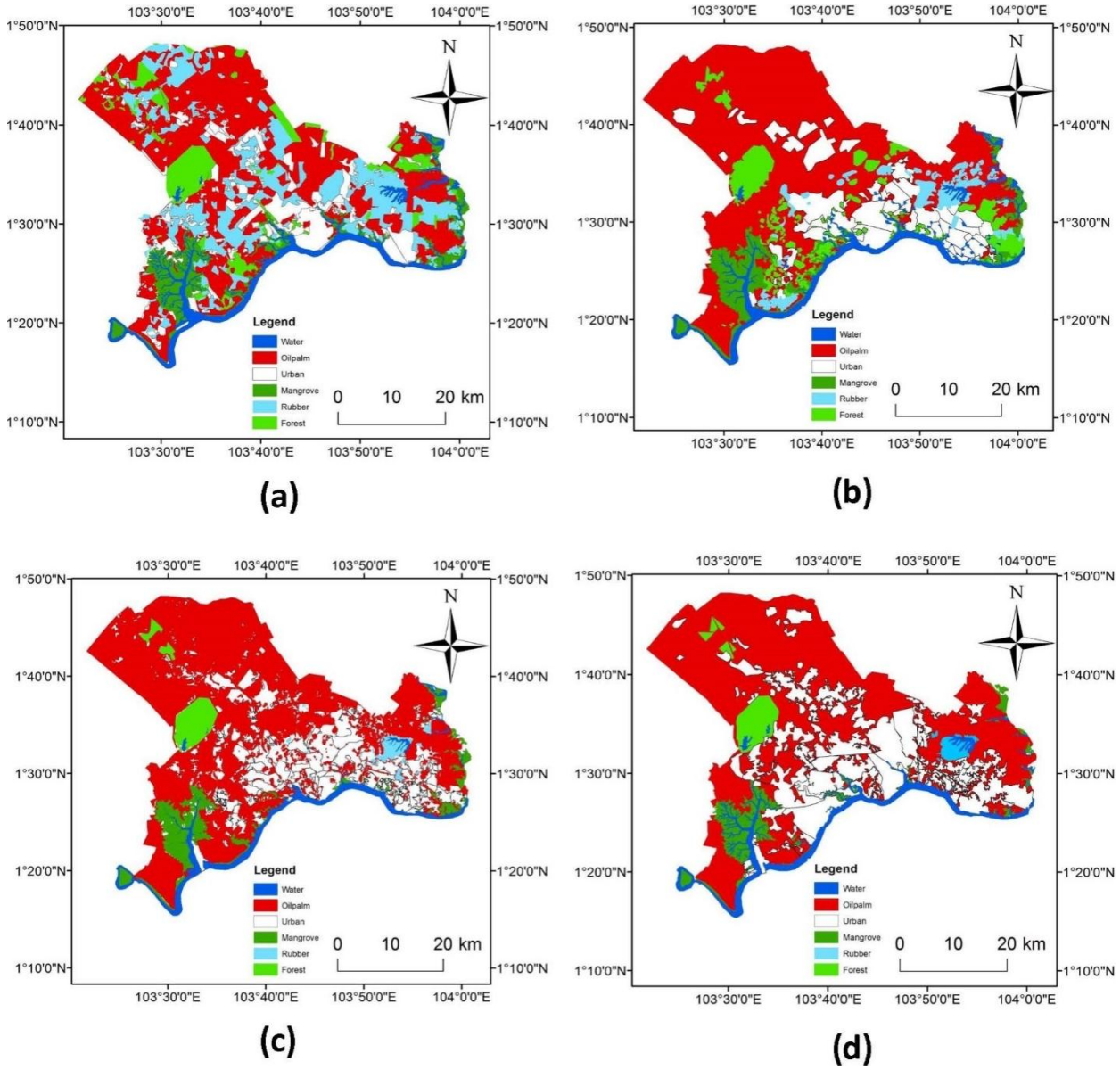

Figure 6. Land use/Land cover classification in Iskandar Malaysia (**a**) 1989; (**b**) 2000; (**c**) 2007; and (**d**) 2014.

Since MLC provided better results in terms of the overall accuracy and had less "salt and pepper" compared to SVM, we selected classification results of MLC for further analysis. Each of the LULC class (as classified using MLC) boundaries was extracted to discard any mixed pixels within the major LULC (Figure 5) and we calculated the total area covered by each of the LULC in each of the Landsat images (Table 3). Figure 6 clearly shows the spatial changes in rubber where in 1989 satellite image rubber plantations dominated the northern part of IM which decreased substantially from 2000 onwards. Rubber plantations were mainly replaced with oil palm plantations and urban surfaces in the northern and southern parts of IM. In Table 3 these LULC areas produced using MLC are compared with the areas from the land use map produced by the Department of Agriculture Malaysia (DOA) and from the Comprehensive Development Plan ii (unpublished). The difference in LULC as estimated by these three different sources produced a Relative predictive error (RPE) of <20% except for the water class in 2013 and 2014 (RPE of −68% and −69% respectively). The large underestimation of the water

class by MLC is because the IRDA has re-defined the boundary of the water from 12,401 ha (2005) to 37,234 ha (2012) (Comprehensive Development Plan ii—unpublished) but our classified images in 2013 and 2014 did not take this into account. Forest and mangrove classes show an overestimation of 16% and an underestimation of 24% respectively in the 2000 image.

4.2. Land Use or Land Cover (LULC) Changes

The LULC changes in IM between 1989 and 2014 were analysed using the results of the MLC classification. The total area covered by each of the six LULC in IM from 1989 to 2014 is shown in Figure 7 and Table 4. In each year oil palm constitutes the largest land area of IM compared to other LULC. In 1989, rubber was the second largest land use type and this was followed by urban, forest and mangrove. This distribution started to change since the beginning of the 1990s where the land used for oil palm plantations increased 43% to 117,715 ha in 2005 and onwards. Urban land use increased steadily from 1989 until 2014 with a rate of 1225 ha per year. Land used for rubber plantation decreased drastically from 46,443 ha in 1989 to only 2043 ha in 2014 (a decrease of 96%). The analysis of satellite images shows that over a period of 25 years IM lost 6740 ha of mangrove areas. However, over the years IM gained 710 ha of mangroves (Figure 8). This resulted in a net loss of 6030 (33%) between 1989 and 2014 or 241 ha per year. The specific locations of mangrove loss and gain between 1989 and 2014 are shown in Figure 8 and Table 5. Action is necessary to protect the existing mangrove cover from further loss. Generally, natural green covers (forest and mangrove) suffered losses of as much as 65% and 33% respectively in 25 years.

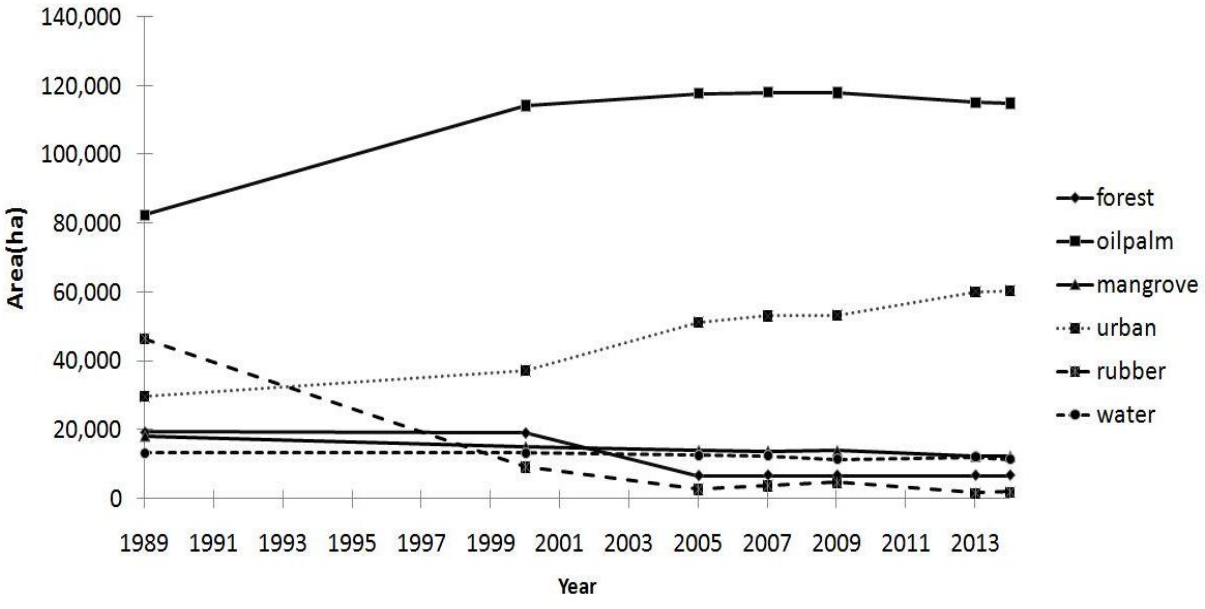

Figure 7. Trend in land cover changes in Iskandar Malaysia since 1989.

Table 4. The percentage (%) change in area by comparing the land use in 2000, 2005, 2007, 2009, 2013 and 2014 with 1989 as a base year. The negative sign shows the % loss in the area compared to 1989 while the positive shows the % gain in the area compared to 1989.

Land Use	1989	2000	2005	2007	2009	2013	2014
Forest	0	−1	−65	−65	−65	−65	−65
Oil Palm	0	38	43	43	43	40	43
Mangrove	0	−18	−24	−25	−24	−32	−33
Urban	0	25	73	78	79	102	103
Rubber	0	−80	−94	−92	−90	−96	−96
Water	0	−1	−5	−6	−13	−9	−13

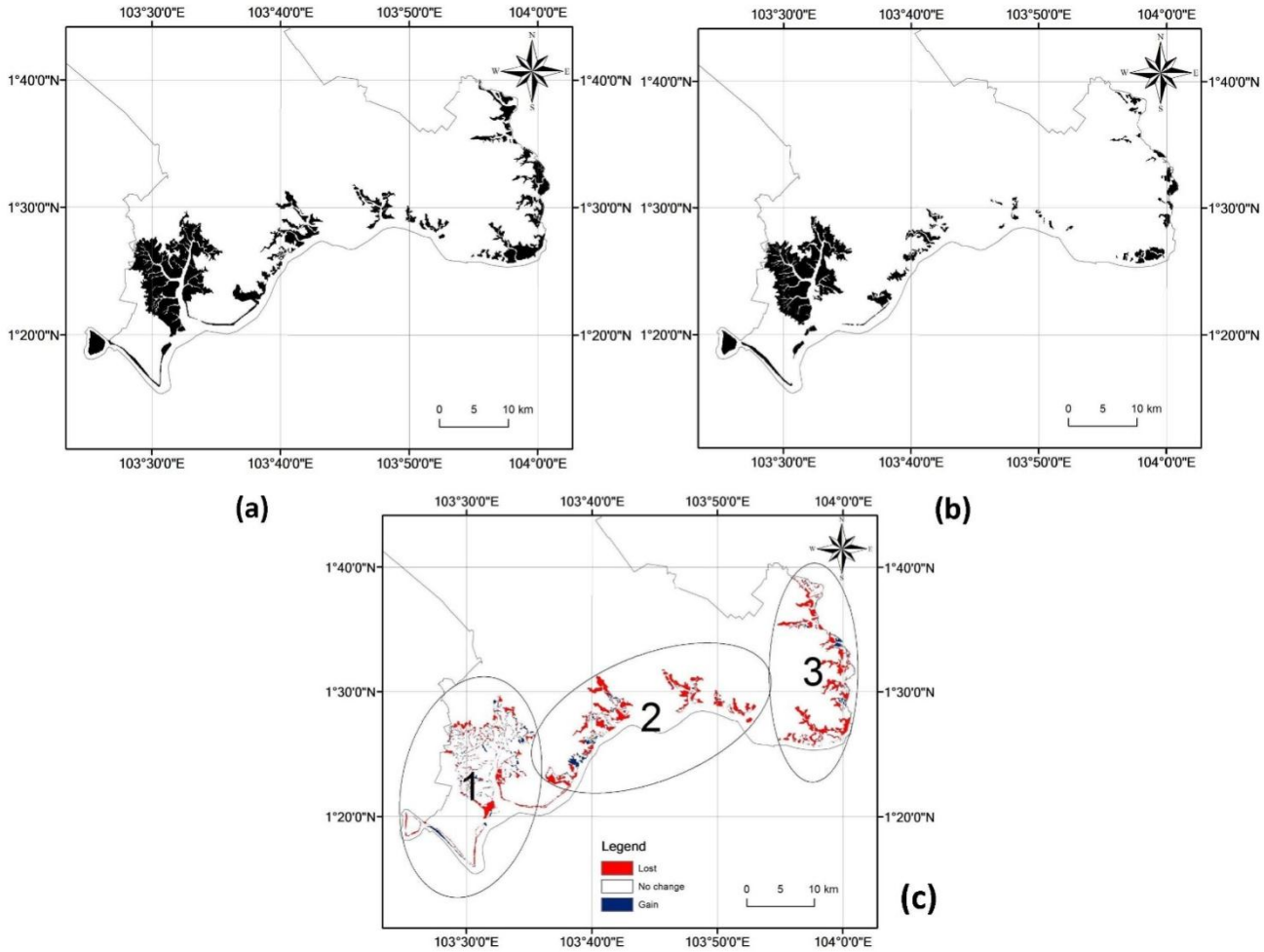

Figure 8. Mangrove cover changes between 1989 and 2014 (**a**) mangrove cover in 1989; (**b**) mangrove cover in 2014; and (**c**) loss and gain of mangrove between 1989 and 2014. The three major mangrove areas are circled and numbered as 1, 2 and 3. Refer to Table 5 for the mangrove areas.

Table 5. Major mangrove sites as shown in Figure 8 in Iskandar Malaysia.

Areas	Location
1	The three Ramsar (Tanjung Piai, Pulau Kukup, and Sungai Pulai) sites that cover 647 ha, 526 ha and 9126 ha of mangroves respectively
2	Pendas Forest and along Pendas, Perepat, Melayu, Skudai, Danga, and Tebrau rivers, Nusajaya, Horizon Hills, Permas Jaya, Masai and Johor Bahru City
3	Along Johor, Serai, and Kong Kong rivers, Pasir Gudang Port and Tanjung Langsat Industrial Area

We verified the locations that we found from satellite images as changed areas (Figure 8) with Google Earth maps (dated 18 November 2010, 16 April 2012, 27 June 2013, 10 February 2014 and 18 February 2015) of IM. The locations that we compared visually with the Google Earth map and whether or not they have changed are shown in Figure 9 and Table 6 respectively. From 18 areas that we compared we found 17 areas were correctly detected by satellite images with MLC classification method as changed and one area (location number 2 in Figure 9) was found to be unchanged while our classification result shows as changed.

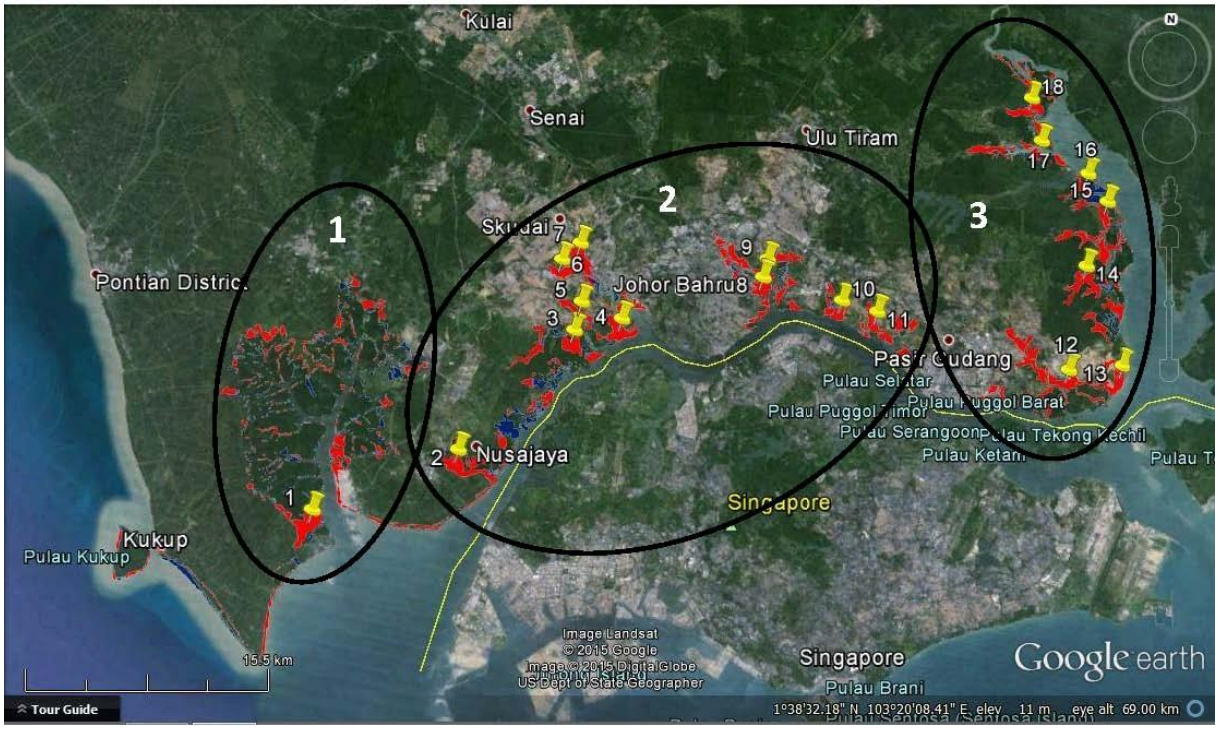

Figure 9. Locations of changed mangrove area as detected from satellite images (red and blue areas refer to mangrove loss and gain, respectively, between 1989 and 2014) overlaid on a Google Earth image. Black circles numbered as 1, 2 and 3 show the major mangrove areas (refer to Table 5) in Iskandar Malaysia. The yellow pincushions show the specific locations of changed mangrove areas that were verified with Google Earth images (refer to Table 6 for the specific locations).

Table 6. Verification of changed mangrove areas as detected by satellite images with Google Earth images.

Point	Place Name/Locations	Lat Long	Areas Corresponding to Figure 7	Change of Land Use
1	ATT Terminal Bin	1 °20′40.47″N 103 °31′47.13″E	1	mangrove to industrial
2	Nusajaya	1 °23′0.21″N 103 °36′43.95″E	1	still mangrove
3	Nusajaya	1 °27′27.41″N 103 °40′37.35″E	2	mangrove to oil palm
4	Taman Laguna	1 °27′57.45″N 103 °42′18.15″E	2	mangrove to residential
5	Kampung Tuah Jaya	1 °28′30.24″N 103 °40′50.00″E	2	mangrove to residential
6	Taman Tampoi Indah	1 °30′40.12″N 103 °40′40.73″E	2	mangrove to residential
7	Taman Perindustrian JB Perdana	1 °30′1.50″N 103 °40′2.86″E	2	mangrove to industrial
8	Taman Perumahan Rakyat Sri Stulang	1 °29′43.16″N 103 °47′18.78″E	2	mangrove to residential
9	Kampung Sri Tasek	1°30′23.92″N 103°47′27.59″E	2	mangrove to residential
10	Senibong Cove	1°29′0.07″N 103°50′12.42″E	2	mangrove to residential
11	Kampung Rekoh	1°28′39.02″N 103°51′28.46″E	2	mangrove to vacant land
12	Kampung Sri Aman	1°26′52.46″N 103°58′18.78″E	3	mangrove to ponds
13	Tanjung Langsat	1°27′7.49″N 104° 0′14.23″E	3	mangrove to industrial
14	Kampung Kong Kong	1°30′41.71″N 103°59′0.65″E	3	mangrove to ponds
15	Hutan Rizab Sg Johor	1°33′8.61″N 103°59′49.73″E	3	mangrove to agricultural land
16	Hutan Rizab Sg Johor	1°34′10.21″N 103°59′8.26″E	3	mangrove to vacant land
17	Jova Resort Sdn Bhd	1°35′23.08″N 103°57′26.75″E	3	mangrove to ponds
18	Nam Heng Estate	1°37′1.07″N 103°57′6.64″E	3	mangrove to oil palm

5. Discussion

5.1. The Choice of Image Classification Algorithms

Many previous studies show that SVM is a better digital image classification technique compared to MLC. About 100 studies conducted using various classification techniques for land cover classification between 2003 and 2010 with high, medium and coarse spatial resolution and hyperspectral remote sensing images reported the superiority of SVM [39]. These studies concluded that SVM is well suited for small training sets and high-dimensional data [43–46]. The use of SVM for mangrove classification was reported by Huang *et al.* [47] and Heumann [48]. Heumann [49] found that the overall accuracy of the SVM classification between true mangroves and mangrove associates was 94.4% and the greatest source of error was the misclassification of mangrove associates as true mangroves. Galvez *et al.* [50] demonstrated the usefulness of SVM for LULC classifications of heterogeneous tropical landscapes. In most of the cases SVM was found to be better than MLC by only a few percentage points (<5%). Jia *et al.* [51] found that SVM is better than MLC by about 1% and SVM could classify croplands better because croplands occurred in aggregated class objects. However, SVM underestimated grasslands because grasslands co-existed with forest and SVM led to the misclassification of grasslands and forest lands. Jia *et al.* [51] attributed the relatively higher accuracy of the SVM technique to its ability to locate an optimal separating hyperplane and generalise the hyperplane using limited training samples to all other unseen pixels in the image and its advantage of no required assumption of any particular data distribution. The use of mixed pixels in the training data sets is also believed to be one of the reasons for SVM to classify LULC with better accuracy compared to the MLC technique.

However, in a seminal paper Li *et al.* [38] studied 15 classification methods on a common set of six bands of Landsat imagery and concluded that the differences between the accuracies of the various methods was really quite small and that in order to achieve an accurate classification it was more important to have a "good" set of training data than to be concerned with which classification method to use. They found that the best classification accuracy using six bands of a Landsat image was achieved by logistic regression, followed by the maximum likelihood classifier (MLC), neural network (NN), support vector machine (SVM), and logistic model tree (LMT) algorithms but the differences in accuracy were quite small. They also concluded that MLC and Logistic regression have superior performances compared to other algorithms as their error range is narrow (using a different number of training samples) and they can be easily set to produce a high accuracy, thus MLC, Logistic Regression (LR), and LMT are the most stable algorithms among all the algorithms.

Although some researchers [43,46,52,53] argue that SVM can produce superior classification results with only a small number of training samples, Li *et al.* [38] showed that when the number of training samples was very small (e.g., 20 and 40 samples), no algorithm performed well, but most of the algorithms achieve their highest accuracies when there are more than 200 samples (pixels) per class. This finding is in contrast to that of Huang *et al.* [52] who argued that fewer spectral bands of a Landsat image and fairly large training samples (2%–20% of entire image) were the reasons for reduced accuracy of SVM compared to ANN. Li *et al.* [38] concluded that most supervised algorithms such as MLC, LR, and LMT could produce high classification accuracies if the parameters are

properly set and training samples are sufficiently representative. The findings of Li *et al.* [38] support the results of our study that MLC with a sufficient number of training samples and their well distributed locations throughout the scene can produce high and stable performance compared to SVM. It is noteworthy that MLC is relatively easy to run and it consumes considerably less computing time (1 min *versus* 10 min for SVM in our study).

Similar to Li *et al.* [38], a few other studies also found the superiority of other classification techniques compared to SVM. Petropoulos *et al.* [53], for example, used both SVM and object-based classification for mapping LULC in the Mediterranean region using Hyperion data. The results of their study showed that the object-based technique had 5% and 6% more overall classification accuracy and kappa coefficient respectively compared to SVM. Similarly, both the producer and user accuracies were also higher for the object-based approach. Otukei and Blaschke [54] found that the decision tree algorithm performed well (3%–4% higher) compared to SVM. Gil *et al.* [55] and Zhang *et al.* [56] found that MLC is better than SVM in classifying plants or land cover using high spatial resolution optical imagery.

As presented in Figure 5, SVM classification resulted in obvious salt and pepper effects compared to MLC even after the clump image post-classification technique was applied on images classified by both algorithms. In low resolution images mixed pixels exist due to the complexity of ground substances, diversity of disturbance, *etc.*, and this spatial autocorrelation of pixels is not commonly considered in the SVM classification, thus causing much noise in the classified images [57]. Similarly Man *et al.* [58] also found that the salt and pepper effect is one of the disadvantages of the SVM technique; they used hyperspectral images for classifying LULC in the University of Houston campus and its neighboring urban area in the southeast of Texas, USA, and the upper part of the Mexico Gulf plains.

5.2. Mangrove Cover Change

The loss of mangroves in Johor for the period of 25 years is estimated at about 6030 ha. As shown in Figure 7 and Table 5, most of the mangroves are found in three sites in IM. The largest loss of mangrove is detected in area 2 (2748 ha), followed by area 3 (2569 ha) and area 1 (1748 ha). Although area 1 has the largest coverage of mangroves in IM (10,299 ha), this site shows relatively least physical disturbance in the last 25 years as compared to the other two areas of study.

Area 1 hosts the three Ramsar sites in Johor, *i.e.*, Kukup island, Tanjung Piai and Sungai Pulai. At present, the former two are the gazetted National Parks managed by the Johor National Parks Corporation while Sungai Pulai is the largest intact mangrove forest reserve under the jurisdiction of Johor Forestry Department. The loss of mangroves in area 1 between 1989 and 2000 was recorded at about 3337 ha or 303 ha per year, but the loss has decreased to 2333 ha (166 ha per year) since 2000. This is believed to be closely associated with the gazetting of Kukup Island and Tanjung Piai as national parks in 1997, and Sungai Pulai as a forest reserve since 1923 and their subsequent designation as Ramsar sites in 2003.

The Ramsar site status recognizes the international importance of these three sites for conserving bio-diversity. However, it is the protected area and forest reserve status that have contributed essentially to the nature conservation of these sites thereby enabling them to support a unique mix of

marine and terrestrial species through providing breeding, feeding and nursery grounds for fish and arthropods, as well as many local and migrant bird species, and reptiles. Mangroves in area 1 are also important for controlling floods and stabilizing shorelines [7].

Despite this significance, development is fast encroaching into these Ramsar sites, especially the Sungai Pulai forest reserve which has not been gazetted as having a protected area status. Its geographical proximity to the development core areas of IM places it under great pressure to be transformed into urban waterfronts and to be cut down for property developments. The controversial massive Forest City project (with a total of estimated 1600 ha reclaimed land area) located at the river mouth of Sungai Pulai will inevitably severely affect the mangrove ecosystem of Sungai Pulai [59].

In earlier years, the construction of Tanjung Pelepas Port and in particular ATT Terminal Bin (Zone C in Figure 2a), which was completed at the end of the 1990s, had substantially contributed to the major loss of mangroves in area 1 (see Table 6). Apart from the human-induced destruction, the intensified erosion rate along the coast has resulted in the shoreline retreat at Tanjung Piai, the southern-most tip of mainland Asia which consists mainly of mudflats and mangrove forests, of which the rate of erosion is between 2 to 4 m·year^{-1} [60]. Moreover, the local hydrodynamic conditions combined with the existence of regular ship wakes, and aquaculture activities, such as in the Sungai Pulai mangrove site, are also believed to be some reasons contributing to the intensive erosion at Tanjung Piai.

Similar to the causes of threat to mangroves in area 1, the mangroves loss in area 2 is closely related to urbanization. Area 2 experienced the most critical condition of mangrove destruction as it is located within the core development area of IM (Zones A and B in Figure 2a). The Danga Bay mixed-use waterfront development project which started in the 1990s has converted nearly the entire mangroves in area 2 into the mixed-use waterfront development. Unlike area 1 and 2, the mangroves in area 3 face the coverage loss mainly due to its conversion into aquaculture activities. The level of destruction is, however, at a lower rate as compared to area 2.

On the other hand, while mangroves were destroyed by anthropogenic activities, replanting efforts have resulted in a gain of 446 ha in the Ramsar sites in area 1 (for every 4.19 ha of mangrove loss a gain of 1 ha has been achieved). Areas 2 and 3 which are not gazetted as either protected areas or forest reserves face substantial loss and relatively lower gain through replanting, at only 183 ha and 81 ha respectively. The ratio of loss to gain in these two areas is 14.1:1 and 28.1:1 respectively. A regular monitoring system needs to be established to control, if not to reverse, the rate of mangrove destruction in Johor.

6. Conclusions

Overall, mangrove areas in Iskandar Malaysia (IM) have decreased at an alarming rate (33%) from 1989 to 2014. The major causes of mangrove destruction in this region are the development of the coastal region (construction of a port, industrial area, water front project, *etc.*), intensified erosion, local hydrodynamic conditions and development of aquaculture activities. On the other hand, a small increase of 710 ha of mangrove occurred in this region and the possible reasons for the gain could be replanting, especially in the Ramsar sites, and regrowth. The loss of about 241 ha per year of

mangroves was associated with a steady increase in urban land use (1225 ha per year) from 1989 until 2014. Action is necessary to protect the existing mangrove cover from further loss.

Systematic monitoring and control measures are urgently needed to protect these sites from further coverage loss in the future. Regular monitoring and mapping can be performed with remote-sensing technology particularly with digital classification techniques. In this study, MLC produced higher overall accuracies and Kappa coefficients and less "salt and pepper effect" compared to SVM for all 7 years of data.

Gazetting of the remaining mangrove sites as protected areas or forest reserves and introducing tourism activities in mangrove areas can ensure the continued survival of mangroves in IM as mangrove forests are valuable ecological and economic resources and they play an important role to ensure economic and environmental sustainability [61].

Therefore, gazetting of the remaining mangrove sites as protected areas or forest reserves at the least can be the basis, with a detailed management plan that indicates the permitted land use activities with different levels of access within these areas is crucial. On the other hand, introducing tourism activities is able to justify the continued conservation of mangroves through the economic values it offers bearing in mind the contribution of tourism to the job opportunities and currency exchange in Malaysia. However, the tourism activities must be carefully planned and centered on environmental education to raise the public awareness of the importance of mangroves, which would later have an influence on the physical development in the region.

Acknowledgments

We acknowledge the Ministry of Education Malaysia (through research grant R.J130000.7301.4B145 and Q.J130000.2427.02G20) for providing funding to conduct the study. We thank the Iskandar Regional Development Authority (IRDA), and Nazarin Ezzaty Mohd Najib for their assistance on this research.

Author Contributions

Kasturi Devi Kanniah supervised the research and wrote the manuscript; Afsaneh Sheikhi, Kian Pang Tan and Fateen Nabilla Rasli processed the data; Hong Ching Goh wrote Section 5.2 of the manuscript; Arthur P. Cracknell and Chin Siong Ho reviewed and edited the manuscript.

Conflicts of Interest

The authors declare no conflict of interest.

References

1. Giri, C.; Ochieng, E.; Tieszen, L.L.; Zhu, Z.; Singh, A.; Loveland, T.; Masek, J.; Duke, N. Status and distribution of mangrove forests of the world using earth observation satellite data. *Glob. Ecol. Biogeogr.* **2011**, *20*, 154–159.
2. Spalding, M.; Kainuma, M.; Collins, L. *World Atlas of Mangroves*, 2nd ed.; Earthscan: London, UK, 2010; p. 350.

3. Dittmar, T.; Hertkorn, N.; Kattner, G.; Lara, R.J. Mangroves, a major source of dissolved organic carbon to the oceans. *Glob. Biogeochem. Cycle* **2006**, *20*, doi:10.1029/2005GB002570.
4. Donato, D.C.; Kauffman, J.B.; Murdiyarso, D.; Kurnianto, S.; Stidham, M.; Kanninen, M. Mangroves among the most carbon-rich forests in the tropics. *Nat. Geosci.* **2011**, *4*, 293–297.
5. Hamdan, O.; Aziz, H.K.; Hasmadi, I.M. L-band ALOS PALSAR for biomass estimation of Matang mangroves, Malaysia. *Remote Sens. Environ.* **2014**, *155*, 69–78.
6. Cornforth, W.A.; Fatoyinbo, T.E.; Freemantle, T.P.; Pettorelli, N. Advanced land observing satellite phased array type L-band SAR (ALOS PALSAR) to inform the conservation of mangroves: Sundarbans as a case study. *Remote Sens.* **2013**, *5*, 224–237.
7. Mubarak, H.T.; Azian, M. Mangroves ecosystem. In *Status of Mangroves in Peninsular Malaysia*; Omar, M., Aziz, K., Shamsudin, I., Raja Barizian, R.S., Eds.; Forest Research Institute Malaysia: Kuala Lumpur, Malaysia, 2012; pp. 11–30.
8. FAO. *The World's Mangroves 1980–2005. A Thematic Study Prepared in the Framework of the Global Forest Resources Assessment 2005*; UN FAO: Rome, Italy, 2007; p. 153.
9. Omar, H. Mangroves threats and changes. In *Status of Mangroves in Peninsular Malaysia*; Omar, M., Aziz, K., Shamsudin, I., Raja Barizian, R.S., Eds.; Forest Research Institute Malaysia: Kuala Lumpur, Malaysia, 2012; pp. 89–110.
10. Polidoro, B.A.; Carpenter, K.E.; Collins, L.; Duke, N.C.; Ellison, A.M.; Ellison, J.C.; Farnsworth, E.J.; Fernando, E.S.; Kathiresan, K.; Koedam, N.E. The loss of species: Mangrove extinction risk and geographic areas of global concern. *PLoS ONE* **2010**, *5*, doi:10.1371/journal.pone.0010095.
11. Kuenzer, C.; Bluemel, A.; Gebhardt, S.; Quoc, T.V.; Dech, S. Remote sensing of mangrove ecosystems: A review. *Remote Sens.* **2011**, *3*, 878–928.
12. Azian, M.; Mubarak, H.T. Functions and values of mangroves. In *Status of Mangroves in Peninsular Malaysia*; Omar, M., Aziz, K., Shamsudin, I., Raja Barizian, R.S., Eds.; Forest Research Institute Malaysia: Kuala Lumpur, Malaysia, 2012; pp. 12–25.
13. Benfield, S.L.; Guzman, H.M.; Mair, J.M. Temporal mangrove dynamics in relation to coastal development in Pacific Panama. *J. Environ. Manag.* **2005**, *76*, 263–276.
14. Manson, F.; Loneragan, N.; Phinn, S. Spatial and temporal variation in distribution of mangroves in Moreton bay, subtropical Australia: A comparison of pattern metrics and change detection analyses based on aerial photographs. *Estuar. Coast. Shelf Sci.* **2003**, *57*, 653–666.
15. Fromard, F.; Vega, C.; Proisy, C. Half a century of dynamic coastal change affecting mangrove shorelines of French Guiana. A case study based on remote sensing data analyses and field surveys. *Mar. Geol.* **2004**, *208*, 265–280.
16. Giri, C.; Long, J.; Abbas, S.; Murali, R.M.; Qamer, F.M.; Pengra, B.; Thau, D. Distribution and dynamics of mangrove forests of South Asia. *J. Environ. Manag.* **2015**, *148*, 101–111.
17. Kamal, M.; Phinn, S. Hyperspectral data for mangrove species mapping: A comparison of pixel-based and object-based approach. *Remote Sens.* **2011**, *3*, 2222–2242.
18. Sulong, I.; Mohd-Lokman, H.; Mohd-Tarmizi, K.; Ismail, A. Mangrove mapping using Landsat imagery and aerial photographs: Kemaman district, Terengganu, Malaysia. *Environ. Dev. Sustain.* **2002**, *4*, 135–152.

19. Satyanarayana, B.; Mohamad, K.A.; Idris, I.F.; Husain, M.-L.; Dahdouh-Guebas, F. Assessment of mangrove vegetation based on remote sensing and ground-truth measurements at Tumpat, Kelantan delta, east coast of Peninsular Malaysia. *Int. J. Remote Sens*. **2011**, *32*, 1635–1650.
20. Liu, Z.; Li, J.; Lim, B.; Seng, C.; Inbaraj, S. Object-based classification for mangrove with VHR remotely sensed image. In Proceedings of the International Conference on Geoinformatics, Remotely Sensed Data and Information, Nanjing, China, 25–27 May 2007.
21. Kanniah, K.D.; Lau, A.M.S.; Rasib, A. Per-pixel and sub-pixel classifications of high-resolution satellite data for mangrove species mapping. *Appl. GIS* **2007**, *3*, 1–22.
22. Pourebrahim, S.; Hadipour, M.; Mokhtar, M.B. Impact assessment of rapid development on land use changes in coastal areas; case of Kuala Langat district, Malaysia. *Environ. Dev. Sustain.* **2014**, *17*, 1003–1016.
23. Hamzah, K.A.; Omar, H.; Ibrahim, S.; Harun, I. Digital change detection of mangrove forest in Selangor using remote sensing and geographic information system (GIS). *Malays. For.* **2009**, *72*, 61–69.
24. Khuzaimah, Z.; Ismail, M.H.; Mansor, S. Mangrove changes analysis by remote sensing and evaluation of ecosystem service value in Sungai Merbok's mangrove forest reserve, Peninsular Malaysia. In *Lecture Notes in Computer Science*, Proceedings of the 13th International Conference in Computational Science and Its Applications–ICCSA. Part II, Ho Chi Minh City, Vietnam, 24–27 June 2013; Springer: Berlin, Germany, 2013; pp. 611–622.
25. Aisyah, A.; Shahrul, A.; Zulfahmie, M.; Mastura, S.S.; Mokhtar, J. Deforestation analysis in Selangor, Malaysia between 1989 and 2011. *J. Trop. For. Sci.* **2015**, *27*, 3–12.
26. Azian, M.; Ismail Adnan, A.; Mohd Hasmadi, I. The use of remote sensing for monitoring spatial and temporal changes in mangrove management. *Malays. For.* **2009**, *72*, 15–22.
27. Hamdan, O.; Khairunnisa, M.; Ammar, A.; Hasmadi, I.M.; Aziz, H.K. Mangrove carbon stock assessment by optical satellite imagery. *J. Trop. For. Sci.* **2013**, *25*, 554–565.
28. Jahari, M.; Khairunniza-Bejo, S.; Shariff, A.R.M.; Shafri, H.Z.M. Change detection studies in Matang mangrove forest area, Perak. *Pertanika J. Sci. Technol.* **2011**, *19*, 307–327.
29. Suratman, M.N.; Ahmad, S. Multi temporal Landsat TM for monitoring mangrove changes in Pulau Indah, Malaysia. In Proceedings of the 2012 IEEE Business, Engineering and Industrial Applications (ISBEIA) Symposium, Bandung, Indonesia, 23–26 September 2012; pp. 163–168.
30. Roslani, M.; Mustapha, M.; Lihan, T.; Juliana, W.W. Applicability of Rapideye satellite imagery in mapping mangrove vegetation species at Matang mangrove forest reserve, Perak, Malaysia. *Environ. Sci. Technol*. **2014**, *7*, 123–136.
31. Kanniah, K.D. Mapping mangrove species using Worldview-2 satellite data. In Proceedings of the 2013, 34th Asian Conference on Remote Sensing, Bali, Indonesia, 20–24 October 2013; pp. 2668–2674.
32. USGS Earth Explorer. Available online: http://earthexplorer.usgs.gov/ (accessed on 5 February 2014).
33. NASA. Landsat 7 Science Data Users Handbook. Available online: http://landsathandbook.gsfc.nasa.gov/pdfs/Landsat7_Handbook.pdf (accessed on 14 February 2014).
34. Sobrino, J.A.; Jiménez-Muñoz, J.C.; Paolini, L. Land surface temperature retrieval from Landsat TM 5. *Remote Sens. Environ*. **2004**, *90*, 434–440.

35. Franya, G.; Cracknell, A. A simple cloud masking approach using NOAA AVHRR daytime data for tropical areas. *Int. J. Remote Sens.* **1995**, *16*, 1697–1705.
36. Song, C.; Woodcock, C.E.; Seto, K.C.; Lenney, M.P.; Macomber, S.A. Classification and change detection using Landsat TM data: When and how to correct atmospheric effects? *Remote Sens. Environ*. **2001**, *75*, 230–244.
37. Coburn, C.; Roberts, A. A multiscale texture analysis procedure for improved forest stand classification. *Int. J. Remote Sens.* **2004**, *25*, 4287–4308.
38. Li, C.; Wang, J.; Wang, L.; Hu, L.; Gong, P. Comparison of classification algorithms and training sample sizes in urban land classification with Landsat thematic mapper imagery. *Remote Sens.* **2014**, *6*, 964–983.
39. Mountrakis, G.; Im, J.; Ogole, C. Support vector machines in remote sensing: A review. *ISPRS J. Photogramm.* **2011**, *66*, 247–259.
40. Atkinson, P.M.; Lewis, P. Geostatistical classification for remote sensing, an introduction. *Comput. Geosci*. **2000**, *26*, 361–371.
41. Chapelle, O.; Haffner, P.; Vapnik, V.N. Support vector machines for histogram-based image classification. *IEEE Trans. Neural Netw*. **1999**, *10*, 1055–1064.
42. Congalton, R.G. A review of assessing the accuracy of classifications of remotely sensed data. *Remote Sens. Environ.* **1991**, *37*, 35–46.
43. Pal, M.; Mather, P. Support vector machines for classification in remote sensing. *Int. J. Remote Sens.* **2005**, *26*, 1007–1011.
44. Dixon, B.; Candade, N. Multispectral Landuse classification using neural networks and support vector machines: One or the other, or both? *Int. J. Remote Sens.* **2008**, *29*, 1185–1206.
45. Karimi, Y.; Prasher, S.; Patel, R.; Kim, S. Application of support vector machine technology for weed and nitrogen stress detection in corn. *Comput. Electron. Agric.* **2006**, *51*, 99–109.
46. Melgani, F.; Bruzzone, L. Classification of hyperspectral remote sensing images with support vector machines. *IEEE Trans. Geosci. Remote Sens.* **2004**, *42*, 1778–1790.
47. Huang, X.; Zhang, L.; Wang, L. Evaluation of morphological texture features for mangrove forest mapping and species discrimination using multispectral IKONOS imagery. *IEEE Trans. Geosci. Remote Sens.***2009**, *6*, 393–397.
48. Heumann, B.W. An object-based classification of mangroves using a hybrid decision tree—Support vector machine approach. *Remote Sens.* **2011**, *3*, 2440–2460.
49. Heumann, B.W. Satellite remote sensing of mangrove forests: Recent advances and future opportunities. *Prog. Phys. Geogr*. **2011**, *35*, 87–108.
50. Paneque-Gálvez, J.; Mas, J.-F.; Moré, G.; Cristóbal, J.; Orta-Martínez, M.; Luz, A.C.; Guèze, M.; Macía, M.J.; Reyes-García, V. Enhanced land use/cover classification of heterogeneous tropical landscapes using support vector machines and textural homogeneity. *Int. J. Appl. Earth Obs.* **2013**, *23*, 372–383.
51. Jia, K.; Wei, X.; Gu, X.; Yao, Y.; Xie, X.; Li, B. Land cover classification using Landsat 8 operational land imager data in Beijing, China. *Geocarto Int.* **2014**, *29*, 941–951.
52. Huang, C.; Davis, L.; Townshend, J. An assessment of support vector machines for land cover classification. *Int. J. Remote Sens.* **2002**, *23*, 725–749.

53. Petropoulos, G.P.; Kalaitzidis, C.; Vadrevu, K.P. Support vector machines and object-based classification for obtaining land-use/cover cartography from hyperion hyperspectral imagery. *Comput. Geosci*. **2012**, *41*, 99–107.
54. Otukei, J.; Blaschke, T. Land cover change assessment using decision trees, support vector machines and maximum likelihood classification algorithms. *Int. J. Appl. Earth Obs. Geoinf.* **2010**, *12*, S27–S31.
55. Gil, A.; Lobo, A.; Abadi, M.; Silva, L.; Calado, H. Mapping invasive woody plants in azores protected areas by using very high-resolution multispectral imagery. *Eur. J. Remote Sens*. **2013**, *46*, 289–304.
56. Zhang, P.; Lv, Z.; Shi, W. Object-based spatial feature for classification of very high resolution remote sensing images. *IEEE Trans. Geosci. Remote Sens*. **2013**, *10*, 1572–1576.
57. Zhang, H.; Shi, W.; Liu, K. Fuzzy-topology-integrated support vector machine for remotely sensed image classification. *IEEE Trans. Geosci. Remote Sens.* **2012**, *50*, 850–862.
58. Man, Q.; Guo, H.; Dong, P.; Liu, G.; Shi, R. Support vector machines and maximum likelihood classification for obtaining land use classification from Hyperspectral imagery. In Proceedings of the International Geoscience and Remote Sensing Symposium (IGARSS), Québec, Canada, 2014; pp. 2878–2881.
59. Low, S.K. DEIA Report Lacks Scientific Data, Says Environmental Activist. Available online: http://www.thesundaily.my/news/1288544 (accessed on 7 January 2015).
60. Awang, N.A.; Jusoh, W.H.W.; Hamid, M.R.A. Coastal erosion at Tanjong Piai, Johor, Malaysia. *Coast. Mar. Sci.* **2014**, *71*, 122–130.
61. Kathiresan, K.; Rajendran, N. Coastal mangrove forests mitigated Tsunami. *Estuar. Coast. Mar. Sci.* **2005**, *65*, 601–606.